

# X-ray Study of Gamma-ray Binaries with Suzaku

Takaaki Tanaka<sup>1</sup>

<sup>1</sup> Kavli Institute for Particle Astrophysics and Cosmology, Stanford University  
*E-mail: ttanaka@slac.stanford.edu*

## ABSTRACT

We report on *Suzaku* observations of two gamma-ray emitting binary systems, LS 5039 and PSR B1259–63. Thanks to its wide band coverage, *Suzaku* has revealed notable temporal/spectral features of the X-ray emission that were not seen by other observatories. From LS 5039 we found that the X-ray emission up to 70 keV is strongly modulating with its orbital period of 3.9 days. For the case of PSR B1259–63, *Suzaku* spectrum shows a break at  $\sim 5$  keV, which allows us to probe the fundamental properties of the pulsar wind.

KEY WORDS: acceleration of particles — X-rays: binaries

## 1. Introduction

Gamma-ray binaries are a new subcategory of X-ray binaries that have been revealed to emit TeV gamma rays or very-high-energy (VHE) gamma rays. Currently, three X-ray binary systems are firmly confirmed as VHE gamma-ray emitters, LS 5039 (Aharonian et al. 2005a), PSR B1259–63 (Aharonian et al. 2005b), and LS I +61° 303 (Albert et al. 2006). An unidentified VHE gamma-ray source, HESS J0632+052, was recently claimed as a candidate for a gamma-ray binary (Hinton et al. 2009). In addition, the MAGIC collaboration reported their detection of Cygnus X-1 during a flare with the post-trial significance of  $4.1 \sigma$  (Albert et al. 2007).

Here we report on results of *Suzaku* observations of two gamma-ray binaries, PSR B1259–63 and LS 5039. To reveal the nature of gamma-ray binary systems, X-rays are expected to be a key wavelength since, most probably, X-rays and VHE gamma-rays are emitted by the same population of electrons via different channels, synchrotron radiation and inverse Compton (IC) scattering, respectively.

PSR B1259–63 is a young radio pulsar (spin period 48 ms) orbiting a B2e star SS 2883 in a highly eccentric 3.4 yr orbit, having spindown power of  $\dot{E}_p \simeq 8 \times 10^{35}$  erg s<sup>-1</sup> (Johnston et al. 1992, 1994; Manchester et al. 1995). PSR B1259–63 was the first example of a radio pulsar forming a binary with a non-degenerate companion (Johnston et al. 1992). Enhanced high-energy emission around periastron which is thought to arise from the interactions between the pulsar wind and the stellar wind/disk, has been observed in X-ray (Kaspi et al. 1995; Hirayama et al. 1996, 1999; Chernyakova et al. 2006) and soft gamma rays (Grove et al. 1995; Shaw et al. 2004). VHE gamma rays have been detected by

the H.E.S.S. telescopes during the periastron passage in 2004 (Aharonian et al. 2005b). The H.E.S.S. lightcurve shows significant variability with strong emission in pre- and post-periastron and with a flux minimum around periastron.

LS 5039 is a high mass X-ray binary (Motch et al. 1997) with extended radio emission (Paredes et al. 2000, 2002). This system is formed by a main-sequence O-type star and a compact object of disputed nature that has been claimed to be both a black hole (e.g., Casares et al. 2005) and a neutron star/pulsar (e.g., Martocchia et al. 2005; Dubus 2006). The compact object is moving around the companion star in a moderately elliptic orbit ( $e = 0.35$ ) with an orbital period of 3.9060 days. LS 5039 has been observed several times in the X-ray energy band (e.g., Bosch-Ramon et al. 2007). Flux variations on timescale of days and sometimes on much shorter timescales have been reported. The spectrum was always well represented by a power law with a photon index of 1.4–1.6. In the VHE domain, the H.E.S.S. collaboration reported their detection and a periodic flux modulation with the orbital period. The VHE flux was found to be at maximum around the inferior conjunction and at minimum around the superior conjunction.

## 2. PSR B1259–63

### 2.1. Data Analysis

We observed the PSR B1259–63 system eight times with the *Suzaku* satellite each with  $\sim 20$  ks exposure in 2007 July, August, and September (Uchiyama et al. 2009). The total exposure time amounts to  $\simeq 170$  ks after standard data screening. We note that this is the first and possibly last chance for *Suzaku* to observe the first disk transit since target visibility does not permit us to ob-

serve it next time.

The most important finding with *Suzaku* would be the presence of a remarkable spectral break by  $\Delta\Gamma \simeq 0.4$  around  $\varepsilon_{\text{br}} \sim 5$  keV at  $\tau \sim -15$  days (the sum of the spectra obtained with third and fourth observations), where  $\tau$  is the days from periastron. Fig. 1 (top) shows the unfolded X-ray spectrum with the best-fit broken power-law model, which gives an statistically acceptable fit. The best-fit photon indices are  $\Gamma_1 = 1.25^{+0.02}_{-0.04}$  and  $\Gamma_2 = 1.66^{+0.05}_{-0.04}$ , with a break energy of  $\varepsilon_{\text{br}} = 4.5^{+0.5}_{-0.2}$  keV. The upper limit on the GSO flux is also plotted in Fig. 1 (top), which strengthens the presence of the spectral steepening.

## 2.2. Discussion

In order to explain the observed spectrum, we performed model calculations within the framework of the shocked relativistic pulsar wind model, in which high-energy radiation comes from shock-accelerated electrons and positrons produced at wind termination shock (e.g., Tavani & Arons 1997). Indeed, the synchrotron and IC radiation by the shock-accelerated  $e^\pm$  pairs from the PSR B1259–63 system as results of the interaction between the relativistic pulsar wind and the Be star outflows have been studied extensively by several authors, and our considerations are based on their works. In the calculations, we assume that distance of the shock from the pulsar,  $r_s$ , is assumed to be much smaller than the star-pulsar separation  $d$ :  $r_s \ll d$  (e.g., Khangulyan et al. 2007).

Unshocked cold  $e^\pm$  pairs in the relativistic wind are assumed to be accelerated at the termination shock and be injected into the downstream postshock flow. The energy distribution of the injected nonthermal  $e^\pm$  pair is described by  $Q(\gamma) = Q_0\gamma^{-p} \exp(-\gamma/\gamma_m)$  for  $\gamma \geq \gamma_1$ , where  $\gamma_1$  is the Lorentz factor of the relativistic wind. A low-energy cutoff with a step function is assumed:  $Q(\gamma) = 0$  for  $\gamma < \gamma_1$ .

The results of the calculation and the *Suzaku* spectrum are shown in the bottom panel of Fig. 1. The observed break energy is related to the Lorentz factor of the pulsar wind:

$$\varepsilon_{\text{br}} = \sqrt{\frac{3}{2}} \frac{e\hbar}{m_e c^2} B \gamma_1^2 \quad (1)$$

$$\simeq 4 \left( \frac{B}{1.8 \text{ G}} \right) \left( \frac{\gamma_1}{4 \times 10^5} \right)^2 \text{ keV}. \quad (2)$$

It is interesting to note that the X-ray spectrum below  $\varepsilon_{\text{br}}$  is predicted to have a universal shape with  $\Gamma = 1$  as long as the cooling is dominated by adiabatic loss and the energy distribution  $Q(\gamma)$  below the low-energy cutoff is harder than  $\gamma^{-1}$ . In fact, the result of the *Suzaku* observations, namely  $\Gamma \simeq 1.2$  immediately below  $\varepsilon_{\text{br}}$ , agrees well with what theoretically expected.

The large magnetic field of  $\sim G$  required to reproduce the data particle acceleration mechanism(s) at work in the termination shock region. Synchrotron cooling time of 10 TeV electrons is about 100 s. To overcome the fast cooling, the acceleration timescale of  $t_{\text{acc}} \sim 100 \text{ s} \sim 50r_L/c$  is necessary at  $E = 10$  TeV, where  $r_L$  denotes the Larmor radius of pairs (see Khangulyan et al. 2007). According to the magnetosonic acceleration model (Hoshino et al. 1992) where the magnetosonic waves collectively emitted by the shock-reflected protons (or heavy ions) are resonantly absorbed by pairs, the inverse of the gyrofrequency of protons with a Lorentz factor of  $\gamma_1$  determines the acceleration timescale; interestingly,  $t_{\text{acc}} \sim m_p c \gamma_1 / (eB) \sim 50 \text{ s}$  is compatible with the requirement posed by our modeling.

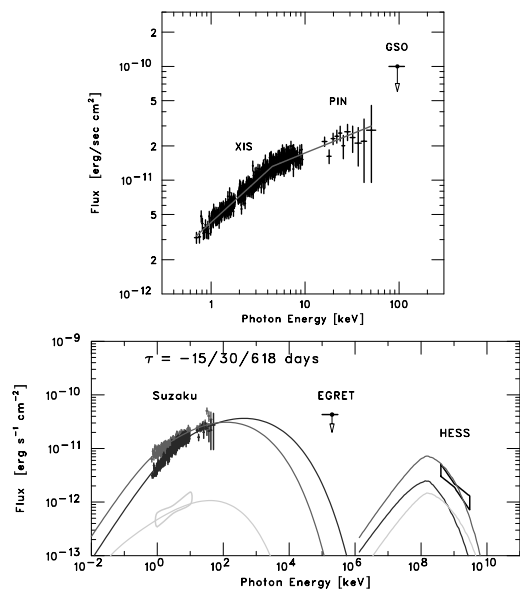


Fig. 1. Top: Broadband X-ray spectra of PSR B1259–63 obtained with *Suzaku* at  $\tau \approx -15$  days. Bottom: Broadband spectra of PSR B1259–63 with the model curves for  $\tau = -15$  days (blue),  $\tau = 30$  days (red), and  $\tau = 618$  days (apastron; green). The X-ray data for apastron is based on *ASCA* results (Hirayama et al. 1999).

## 3. LS 5039

### 3.1. Data Analysis

The temporal and spectral characteristics of the X-ray emission from LS 5039 along the orbit should give us important clues for understanding the acceleration/radiation processes in this source. Therefore, we performed a long,  $\sim 200$  ks observation with the *Suzaku* X-ray observatory, which gives us an unprecedented coverage of more than one orbital period, continuously from 2007 September 9 to 15 (Takahashi et al. 2009).

The XIS lightcurve is shown in the top panel of Fig. 2. The continuous coverage in X-rays, longer than the or-

bit period of the LS 5039 system, reveals a smooth variation of a factor 2 in the 1–10 keV count rate. The lightcurve is drawn over two orbital periods. The orbital phase is calculated with the period of 3.90603 days, and  $\phi = 0$  with reference epoch  $T_0$  ( $\text{HJD} - 2400000.5 = 51942.59$ ) (Casares et al. 2005). The lightcurve from phase  $\phi = 1.0$  to 1.5, which was obtained in the last part of the observation, smoothly overlaps with the one obtained at the beginning of the observation ( $\phi = 0.0$ –0.5).

In the middle panel of Fig. 2, we present the lightcurve obtained with the HXD-PIN for the energy range 15–40 keV. Although the statistical errors are larger, the modulation behavior is similar to that of the XIS. The amplitude of the modulation is roughly the same between the XIS and HXD-PIN, indicating small changes of spectral shapes depending on orbital phase. The spectral parameters obtained for each orbital phase are reported in the following section. The lightcurves obtained with *Suzaku* show that the X-ray flux minimum appears around phase 0.0–0.3 and it reaches maximum around phase 0.5–0.8. This is similar to the structure discovered in the phase diagram of integral fluxes at energies  $> 1$  TeV obtained on a run-by-run basis from H.E.S.S. data (2004 to 2005) (Aharonian et al. 2006).

The *Suzaku* spectrum of LS 5039 shows featureless continuum. The phase-averaged spectrum from 0.7–70 keV is well fitted with an absorbed power law with a photon index of  $\Gamma = 1.51 \pm 0.02$ . We also investigated spectral characteristics at each orbital phase by dividing the data into phase segments of  $\Delta\phi = 0.1$ . Each spectrum is well fitted with absorbed power laws with photon indices ranging from  $\Gamma = 1.45$  to  $\Gamma = 1.61$ . The spectral shape varied such that the spectrum is steep around superior conjunction ( $\Gamma \simeq 1.6$ ) and becomes hard ( $\Gamma \simeq 1.45$ ) around apastron.

### 3.2. Discussion

The X-ray emission observed with *Suzaku* is characterized by (1) a hard power law with  $\Gamma \simeq 1.5$  extending from soft X-rays to  $\sim 70$  keV, (2) clear orbital modulation in flux and photon index, (3) a moderate X-ray luminosity of  $L_X \sim 10^{33}$  erg s $^{-1}$ , and (4) lack of detectable emission lines. Those spectral characteristics in favor a synchrotron origin of the X-rays, which is also supported by the general similarities between the properties of the observed X-rays and TeV gamma-rays.

In currently favored interpretations, TeV gamma rays are produced by IC scattering of the photon field of the massive companion star. Assuming that the TeV gamma-ray production region is located at a distance from the companion star of  $d \sim 2 \times 10^{12}$  cm (i.e. the binary system size), and taking into account that gamma rays are produced in deep Klein-Nishina (KN) regime, for the well known luminosity of the optical star  $L \simeq 7 \times 10^{38}$  erg s $^{-1}$ , one can estimate quite robustly the

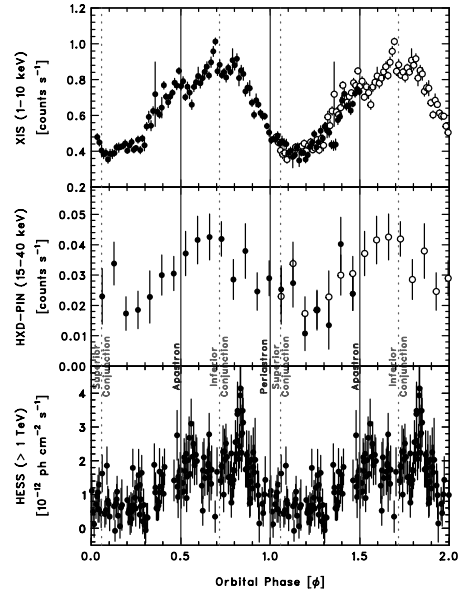


Fig. 2. Orbital lightcurves of LS 5039. Top: XIS (1–10 keV). Middle: HXD (15–40 keV). Bottom: H.E.S.S. ( $> 1$  TeV) (Aharonian et al. 2006)

strength of the emitter magnetic field to be around a few Gauss. For such a magnetic field strength, the energy intervals of electrons responsible for the X-rays and TeV gamma rays largely overlap.

Fig. 3 shows the synchrotron and IC cooling times of electrons, as a function of the electron energy calculated for the stellar photon density at  $d = 2 \times 10^{12}$  cm and for a magnetic field  $B = 3$  G. To understand better the energy intervals of electrons responsible for X-rays and gamma rays, we show the energy zones of electrons relevant to the *Suzaku*, *Fermi*-LAT, and H.E.S.S. radiation domains. It is seen that synchrotron losses dominate over IC ones at  $E_e \geq 1$  TeV. Note also that the TeV gamma-ray production takes place in the deep KN regime while the GeV gamma rays are produced via IC scattering in the Thomson regime.

Formally, when X-rays and TeV gamma-rays are produced by the same population of very high energy electrons, one should expect a general correlation between the lightcurves obtained by *Suzaku* and H.E.S.S. In this case, however, such an interoperation is not valid, since the main mechanisms responsible for the TeV gamma-ray modulation are considered to be anisotropic IC scattering and photon-photon pair production, (Khangulyan et al. 2008; Dubus et al. 2008), both of which cannot contribute the X-ray modulation. This modulation requires periodic changes of the strength of the ambient magnetic field or number of relativistic electrons. Note, however, that the change of magnetic field would not have a strong impact as long as the radiation proceeds

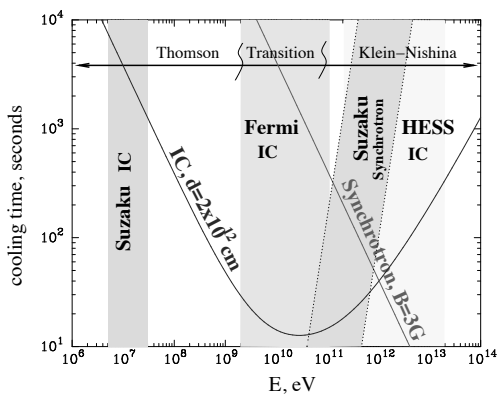


Fig. 3. Radiative cooling times as a function of electron energy calculated with parameters expected for LS 5039.

in the saturation regime and synchrotron losses dominate in the relevant energy interval.

A more natural reason for the modulation of the synchrotron fluxes would come from dominant adiabatic losses. In the regime dominated by adiabatic energy losses, the synchrotron X-ray flux is proportional to  $t_{\text{ad}}$ . The X-ray modulation is then described by the modulation of the adiabatic loss rate. In Fig. 4, we show  $t_{\text{ad}}(\phi)$ , i.e. the orbital modulation of the adiabatic cooling time as inferred from the X-ray data. As seen from the plot, the required adiabatic cooling times are  $\sim 1$  s. Fig. 4 also shows lightcurves of X-ray and gamma-ray emission calculated by our model. Note that those curves explain well the X-ray and VHE gamma-ray data as well as recently published *Fermi*-LAT data (Abdo et al. 2009). The adiabatic loss rate can be written as:  $b_{\text{ad}}(\phi, \gamma) = \gamma/t_{\text{ad}}$  with  $t_{\text{ad}} \sim R/c \simeq 3R_{11}$  s, where  $R_{11} \equiv R/(10^{11} \text{ cm})$  is the characteristic size of the source. Thus the required variation of the adiabatic cooling is reduced to the modulation of the size of the radiation region ( $R_{11} \sim 0.3\text{--}1$ ). The size in its turn depends on the external pressure exerted by, e.g., the stellar wind from the massive star. The expected weaker external pressure around apastron implicitly assumed in our model would be broadly consistent with the radial dependence of the wind pressure.

The fast adiabatic losses impose a strong constraint on the acceleration rate of electrons. Indeed, the acceleration timescale can be expressed as:  $t_{\text{acc}} = \eta R_L/c \sim 0.1\eta(E_e/1\text{TeV})(B/1\text{G})^{-1}$  s, where  $\eta \geq 1$  parametrizes the acceleration efficiency. In the extreme accelerators with the maximum possible rate allowed by classical electrodynamics  $\eta = 1$ . The H.E.S.S. spectrum provides evidence of electron acceleration well above 10 TeV. Therefore,  $t_{\text{acc}} < t_{\text{ad}} \sim 1$  s is required at  $E_e = 10$  TeV, which translates into  $\eta < 3$  for  $B = 3$  G. Thus we arrive at the conclusion that an extremely efficient acceleration with  $\eta < 3$  should operate in a compact region of  $R \sim 10^{11}$  cm.

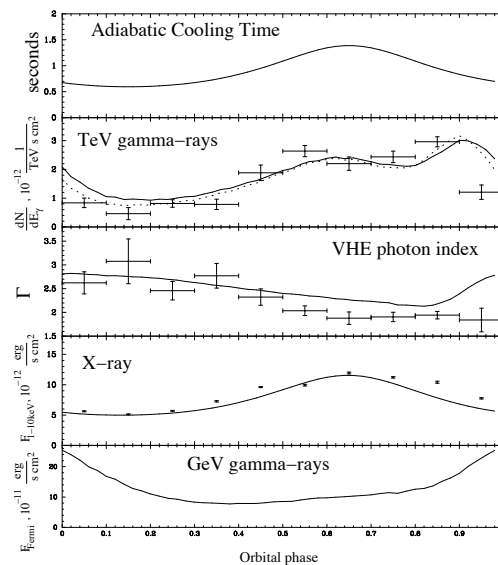


Fig. 4. Lightcurves predicted by our model. The X-ray and VHE gamma-ray data are from *Suzaku* and H.E.S.S. (Aharonian et al. 2006), respectively.

## References

- Abod, A. A., et al. 2009, *ApJ*, 706, L56  
 Aharonian, F. A., et al. 2005a, *Science*, 309, 746  
 Aharonian, F. A., et al. 2005b, *A&A*, 442, 1  
 Aharonian, F. A., et al. 2006, *A&A*, 460, 743  
 Albert, J., et al. 2006, *Science*, 312, 1771  
 Albert, J., et al. 2007, *ApJ*, 665, L1  
 Bosch-Ramon, V., et al. 2007, *A&A*, 473, 545  
 Casares, J., et al. 2005, *MNRAS*, 364, 899  
 Dubus, G. 2006, *A&A*, 456, 801  
 Dubus, G., et al. 2008, *A&A*, 477, 691  
 Grove, J. E., et al. 1995, *ApJ*, 447, L113  
 Hinton, J. A., et al. 2009, *ApJ*, 690, L101  
 Hirayama, M., et al. 1996, *PASJ*, 48, 833  
 Hirayama, M., et al. 1999, *ApJ*, 521, 718  
 Hoshino, M., et al. 1992, *ApJ*, 390, 454  
 Johnston, S., et al. 1992, *ApJ*, 387, L37  
 Johnston, S., et al. 1994, *MNRAS*, 268, 430  
 Kaspi, V. M., et al. 1995, *ApJ*, 453, 424  
 Khangulyan, D., et al. 2007, *MNRAS*, 380, 320  
 Khangulyan, D., et al. 2008, *MNRAS*, 383, 467  
 Manchester, R. N., et al. 1995, *ApJ*, 445, L137  
 Martocchia, A., et al. 2005, *A&A*, 430, 245  
 Motch, C., et al. 1997, *A&A*, 323, 853  
 Paredes, J. M., et al. 2000, *Science*, 288, 2340  
 Paredes, J. M., et al. 2002, *A&A*, 393, L99  
 Shaw, S. E., et al. 2004, *A&A*, 426, L33  
 Tavani, M., & Arons, J. 1997, *ApJ*, 477, 439  
 Takahashi, T., et al. 2009, *ApJ*, 697, 592  
 Uchiyama, Y., et al. 2009, *ApJ*, 698, 911